

**ESTIMATION OF ORBITAL NEUTRON DETECTOR SPATIAL RESOLUTION BY SYSTEMATIC SHIFTING OF DIFFERENTIAL TOPOGRAPHIC MASKS.** T.P. McClanahan<sup>1</sup>, I.G. Mitrofanov<sup>2</sup>, W.V. Boynton<sup>3</sup>, G. Chin<sup>1</sup>, T. Livengood<sup>1</sup>, R.D. Starr<sup>4</sup>, L.G. Evans<sup>5</sup>, G. Neumann<sup>1</sup>, E. Mazarico<sup>1,6</sup>, D. E. Smith<sup>6</sup>, The LEND and LOLA Teams\*, Astrochemistry Laboratory, NASA Goddard Space Flight Center, Greenbelt, MD 20771, ([timothy.p.mcclanahan@nasa.gov](mailto:timothy.p.mcclanahan@nasa.gov)), <sup>2</sup>Institute for Space Research, RAS, Moscow 117997, Russia, <sup>3</sup>Lunar and Planetary Laboratory, Univ. of Arizona, Tucson AZ, <sup>4</sup>Catholic Univ. of America, Washington DC, <sup>5</sup>Computer Sciences Corporation, Lanham MD 20706, <sup>6</sup>Dept. of Earth, Atmos., and Planet. Sci., MIT, Cambridge, MA, USA.

**Introduction:** We present a method and preliminary results related to determining the spatial resolution of orbital neutron detectors using epithermal maps and differential topographic masks. Our technique is similar to coded aperture imaging methods for optimizing photonic signals in telescopes [1]. In that approach photon masks with known spatial patterns in a telescope aperture are used to systematically restrict incoming photons which minimizes interference and enhances photon signal to noise.

Three orbital neutron detector systems with different stated spatial resolutions are evaluated. The differing spatial resolutions arise due different orbital altitudes and the use of neutron collimation techniques. 1) The uncollimated Lunar Prospector Neutron Spectrometer (LPNS) system has spatial resolution of 45km FWHM from ~30km altitude mission phase [2]. The Lunar Renaissance Orbiter (LRO) Lunar Exploration Neutron Detector (LEND) with two detectors at 50km altitude evaluated here: 2) the collimated 10km FWHM spatial resolution detector CSETN and 3) LEND's collimated Sensor for Epithermal Neutrons (SETN). Thus providing two orbital altitudes to study factors of: uncollimated vs collimated and two average altitudes for their effect on fields-of-view.

**Background:** In prior research we identified the existence of a statistically significant epithermal rate contrast between pole-facing and equator-facing slopes using correlated LEND and LOLA maps [5-6]. The study entailed a systematic, bulk decomposition of the maps in latitudes,  $\pm 65^\circ$  to poles to identify highly sloped  $> 5^\circ$ , poleward and equator-facing slopes. To obtain these regions we transformed the LOLA topography to delineate and classify regions as sparsely distributed, equator-facing **EF** and pole-facing **PF** sets of spots. Over each spot we calculated the epithermal average count rates. Using statistical t-tests, we determined the difference in the class means ( $\mu_{EF} - \mu_{PF}$ ) was consistently and significantly positive over several regions,  $\sim 0.01$ cps for both poles. Figure 1 illustrates equator-facing **EF** (red) and pole-facing **PF** (blue) spots for the South pole,  $-80^\circ$  to pole. Importantly, the unique spatial locations and delineations of these spots define our differential topographic mask utilized in the following experiments.

We have further validated our epithermal contrast results by observing similar significant epithermal contrasts using the uncollimated LPNS and SETN maps that were prepared identically to those described. Importantly, this result implies neutron collimation is not required for the observation of epithermal contrast.

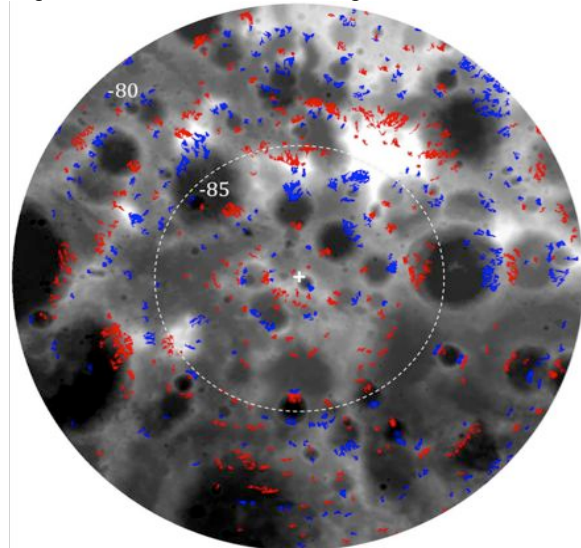


**Figure 1:** LOLA south pole centered DEM [8], ( $-80^\circ$ - $90^\circ$ ). Elevation (greyscale). High slopes  $> 5^\circ$  (color). Pole-facing spots **PF** (blue), Equator-facing spots **EF** (red). We systematically rotate the epithermal maps relative to the topography and determine the epithermal contrasts (**EF** - **PF**) at each  $1^\circ$  rotation.

**Methods:** We tested the robustness of the LEND and LPNS epithermal contrasts  $\pm 65^\circ$  to poles by systematically rotating over  $360^\circ$  the epithermal maps vs. the fixed position differential topographic mask. At each rotation position we evaluated the epithermal contrast. Full registration of the maps occurs only at rotation position 0, thus all other rotation positions are misregistered. As a result any epithermal contrast in the non-0 positions is random. **Hypothesis 1:** the epithermal contrast should be significantly maximized at rotation position 0. **Hypothesis 2:** Assuming *H1* is valid, then by systematically evaluating the epithermal contrast within in small incremental rotations less than the detector field-of-view's range from position 0, we may quantify the relative width of the impulse response. From the width of the impulse response we may infer the instrument spatial resolution. This hypothesis has its roots in convolution theory, where the

width of the impulse response is related to the spatial width of the patterns used in the convolution. In this process the topographic masks are fixed and known and the other convolving structure is the unknown instrument field-of-view.

**Results:** *Hypothesis 1*) In Figs. 2 and 3 we illustrate the epithermal contrasts derived by rotating the epithermal maps relative to the topographic masks for a full 360 degrees, in 1° increments. At each rotation position we determined the epithermal contrast. For LEND and LPNS both polar (4) results indicate a maximum and significant epithermal contrast at rotation position 0 (maps registered). We determined the combined epithermal contrast standard deviations  $\sigma$  from rotation positions [-180:-30 and 210: 360] and normalized the epithermal contrasts found at rotation position 0, yielding significances [LEND SP = 4.72 $\sigma$ , LEND NP = 3.9 $\sigma$ , LPNS SP = 8.07 $\sigma$ , LPNS NP = 4.36 $\sigma$ ] which further validates the epithermal contrast observations.

*Hypothesis 2*) To test the angular width of the impulse response we systematically rotated the epithermal maps between -10° and 10° of rotation position 0, in 0.25° increments. Figure 4 illustrates the epithermal contrast, impulse response for the 3 detectors system and pole. Plots are normalized to illustrate the FWHM at intensity = 0.5.

Detector System	FWHM°	Det Avg FWHM°	Avg/(LEND Coll Avg)
LEND Coll SP	5.25	3.88	1
LEND Coll NP	2.5		
LPNS UnColl SP	7	7.88	2.03
LPNS UnColl NP	8.75		
LEND UnColl SP	11	10.5	2.71
LEND UnColl NP	10		

Our preliminary results indicate, using detector averages, normalized by LEND's collimated FWHM, we find LPNS is ~2.03 times LEND's uncollimated avg, SETN FWHM is ~2.7 times LEND uncollimated. Further, in Fig 4, SETN is not strongly converged to rotation position 0 for either pole and may be too high to detect the EF and PF spots. LEND SETN has a 66% higher altitude than LPNS and a 33% larger FWHM estimate, consistent with the fractional change in visible lunar area 29% and commensurate increased blurring. From this correlated evidence, we suggest the LEND collimated detector's field-of-view is narrower than LPNS.

A draw back to the present approach is related to the non-uniform displacement of the epithermal map pixels relative to the topography in the present rotational scheme, so we do not further quantify the field-of-view estimates. Our objectives over the coming months will be to model the present detector systems and establish

techniques for evaluation that may better quantify the instrument fields-of-view.

**References:** [1] Caroli *et al.*, *Sp. Sci. Rev.* #45 (1987) [2] Feldman *et al.* (1998) *Science* #281 [3] Chin *et al.* (2007) *Sp. Sci. Rev.* #150 [4] Mitrofanov *et al.* (2007) *Sp. Sci. Rev.* #150 [5] Smith *et al.* (2007) *Sp. Sci. Rev.* #150 [6] McClanahan *et al.*, (2011) *A Wet vs. Dry Moon, Conf. Proc.*

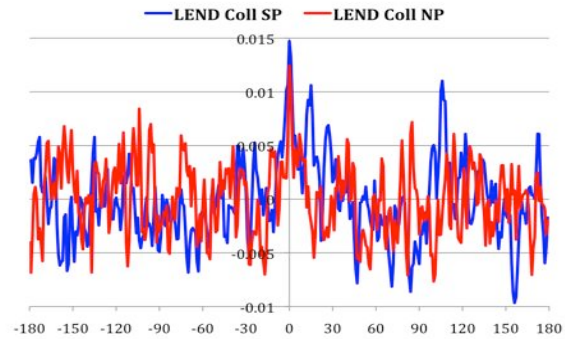


**Figure 2.** LEND Epithermal contrasts determined in 1° increments for 360 degrees of rotation of the epithermal maps vs. topographic masks. North (NP) and South (SP) epithermal contrasts derived in each region, ±65° to poles illustrated. Only at position 0 are the epi and topo maps fully registered.

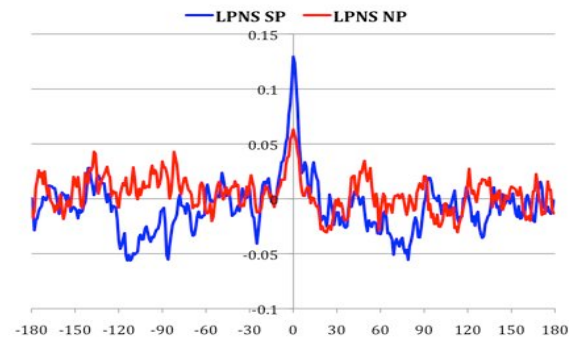


**Figure 3.** LPNS Epithermal contrasts using identical configurations and topographic masks as used in Fig 2.

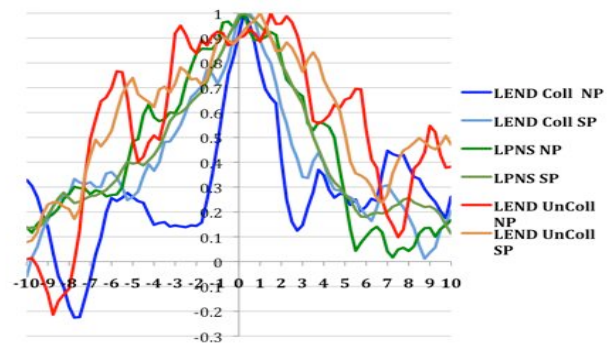


**Figure 4:** LEND and LPNS normalized epithermal contrasts derived by rotating the epithermal map within -10° to +10° of the topographic masks in 0.25° increments. Results suggest LEND collimated has a narrower impulse response FWHM than LPNS for both poles.